Active-grating monochromator for the spectral selection of ultrashort pulses

Fabio Frassetto,[1,*] Stefano Bonora,[1,4] Caterina Vozzi,[2] Salvatore Stagira,[2] Erika Zanchetta,[3] Gioia Della Giustina,[3] Giovanna Brusatin,[3] and Luca Poletto[1]

[1]*National Council for Research of Italy - Institute of Photonics and Nanotechnologies, via Trasea 7, 35131 Padova, Italy*

[2]*Department of Physics - Politecnico di Milano and National Council for Research of Italy - Institute of Photonics and Nanotechnologies, P.zza L. Da Vinci 32, 20133 Milano, Italy*

[3]*Industrial Engineering Department, University of Padova, Via Marzolo 9, 35131 Padova, Italy*

[4]*bonox@dei.unipd.it*

[*]*frassett@dei.unipd.it*

Abstract: Active gratings have been used to realize a grazing-incidence double-grating monochromator for the spectral selection of ultrashort pulses while preserving the temporal duration by compensating for the pulse-front tilt. The active grating consists of a bimorph deformable mirror on the top of which a diffraction grating with laminar profile is realized by UV lithography. The time-delay compensated configuration has been tested with ultrashort pulses at 800 nm. The feasibility of this configuration for the extreme-ultraviolet spectral region has been demonstrated by ray tracing studies.

OCIS codes: (050.1950) Diffraction gratings; (220.1080) Active or adaptive optics; (190.4160) Multiharmonic generation; (320.5520) Pulse compression.

References and links

1. P. Jaeglè, *Coherent Sources of XUV Radiation,* (Springer, 2006).
2. F. Krausz and M. Ivanov, "Attosecond physics," Rev. Mod. Phys. **81**(1), 163–234 (2009).
3. G. Sansone, L. Poletto, and M. Nisoli, "High-energy attosecond light sources," Nat. Photonics **5**(11), 655–663 (2011).
4. T. Sekikawa, T. Okamoto, E. Haraguchi, M. Yamashita, and T. Nakajima, "Two-photon resonant excitation of a doubly excited state in He atoms by high-harmonic pulses," Opt. Express **16**(26), 21922–21929 (2008).
5. W. Li, X. Zhou, R. Lock, S. Patchkovskii, A. Stolow, H. C. Kapteyn, and M. M. Murnane, "Time-resolved dynamics in N_2O_4 probed using high harmonic generation," Science **322**(5905), 1207–1211 (2008).
6. H. Wang, M. Chini, S. Chen, C.-H. Zhang, F. He, Y. Cheng, Y. Wu, U. Thumm, and Z. Chang, "Attosecond time-resolved autoionization of argon," Phys. Rev. Lett. **105**(14), 143002 (2010).
7. L. Poletto and F. Frassetto, "Time-preserving grating monochromators for ultrafast extreme-ultraviolet pulses," Appl. Opt. **49**(28), 5465–5473 (2010).
8. L. Poletto, F. Frassetto, and P. Villoresi, "Ultrafast Grating Instruments in the Extreme Ultraviolet," J. Sel. Top. Quantum Electron. **18**(1), 467–478 (2012).
9. P. Villoresi, "Compensation of optical path lengths in extreme-ultraviolet and soft-x-ray monochromators for ultrafast pulses," Appl. Opt. **38**(28), 6040–6049 (1999).
10. L. Poletto, "Time-compensated grazing-incidence monochromator for extreme-ultraviolet and soft X-ray high-order harmonics," Appl. Phys. B **78**(7-8), 1013–1016 (2004).
11. L. Nugent-Glandorf, M. Scheer, D. A. Samuels, V. Bierbaum, and S. R. Leone, "A laser-based instrument for the study of ultrafast chemical dynamics by soft x-ray-probe photoelectron spectroscopy," Rev. Sci. Instrum. **73**(4), 1875 (2002).
12. J. Norin, K. Osvay, F. Albert, D. Descamps, J. Yang, A. Lhuillier, and C.-G. Wahlström, "Design of an extreme-ultraviolet monochromator free from temporal stretching," Appl. Opt. **43**(5), 1072–1081 (2004).
13. M. Ito, Y. Kataoka, T. Okamoto, M. Yamashita, and T. Sekikawa, "Spatiotemporal characterization of single-order high harmonic pulses from time-compensated toroidal-grating monochromator," Opt. Express **18**(6), 6071–6078 (2010).
14. H. Igarashi, A. Makida, M. Ito, and T. Sekikawa, "Pulse compression of phase-matched high harmonic pulses from a time-delay compensated monochromator," Opt. Express **20**(4), 3725–3732 (2012).
15. L. Poletto and P. Villoresi, "Time-delay compensated monochromator in the off-plane mount for extreme-ultraviolet ultrashort pulses," Appl. Opt. **45**(34), 8577–8585 (2006).

#185565 - $15.00 USD Received 19 Feb 2013; revised 11 Mar 2013; accepted 11 Mar 2013; published 20 May 2013

16. L. Poletto, P. Villoresi, E. Benedetti, F. Ferrari, S. Stagira, G. Sansone, and M. Nisoli, "Intense femtosecond extreme ultraviolet pulses by using a time-delay-compensated monochromator," Opt. Lett. **32**(19), 2897–2899 (2007).
17. L. Poletto, P. Villoresi, F. Frassetto, F. Calegari, F. Ferrari, M. Lucchini, G. Sansone, and M. Nisoli, "Time-delay compensated monochromator for the spectral selection of extreme-ultraviolet high-order laser harmonics," Rev. Sci. Instrum. **80**(12), 123109 (2009).
18. O. Solgaard, F. S. A. Sandejas, and D. M. Bloom, "Deformable grating optical modulator," Opt. Lett. **17**(9), 688–690 (1992).
19. C. W. Wong, Y. Jeon, G. Barbastathis, and S. G. Kim, "Analog tunable gratings driven by thin-film piezoelectric microelectromechanical actuators," Appl. Opt. **42**(4), 621–626 (2003).
20. R. A. Guerrero, M. W. C. Sze, and J. R. A. Batiller, "Deformable curvature and beam scanning with an elastomeric concave grating actuated by a shape memory alloy," Appl. Opt. **49**(19), 3634–3639 (2010).
21. S.-J. Chen, C. T. Chen, S. Y. Perng, C. K. Kuan, T. C. Tseng, and D. J. Wang, "Design and fabrication of an active polynomial grating for soft-X-ray monochromators and spectrometers," Nucl. Instrum. Methods Phys. Res. A **467**, 298–301 (2001).
22. H. S. Fung, J. Y. Yuh, L. J. Huang, T. C. Tseng, S. Y. Perng, D. J. Wang, K. L. Tsang, and S. C. Chung, "A Soft X-Ray (300-1000 eV) Active Grating Monochromator Beamline at NSRRC," Ninth International Conference on Synchrotron Radiation Instrumentation AIP Conf. Proc. **879**, 563–566 (2007).
23. S. Bonora, F. Frassetto, E. Zanchetta, G. Della Giustina, G. Brusatin, and L. Poletto, "Active Diffraction Gratings: Development and Tests," Rev. Sci. Instrum. **83**(12), 123106 (2012).
24. R. Trebino, K. W. DeLong, D. N. Fittinghoff, J. N. Sweetser, M. A. Krumbugel, B. A. Richman, and D. J. Kane, "Measuring ultrashort laser pulses in the time-frequency domain using frequency-resolved optical gating," Rev. Sci. Instrum. **68**(9), 3277 (1997).
25. C. Radzewicz, J. S. Krasinski, M. J. la Grone, M. Trippenbach, and Y. B. Band, "Interferometric measurement of femtosecond wave-packet tilting in rutile crystal," J. Opt. Soc. Am. B **14**(2), 420–424 (1997).

1. Introduction

High-order harmonic (HH) generation driven by ultrashort laser pulses in gases is widely recognized as an effective way to realize coherent, brilliant, ultrashort table-top sources in the extreme ultraviolet (XUV) and soft x-ray regions [1] that can be exploited for time-resolved spectroscopy of matter with sub-femtosecond resolution [2–6]. For some spectroscopic application the spectral selection of a single harmonic is required and should be accomplished by a suitable monochromator able to preserve the shortest temporal duration allowed by the selected spectral bandwidth of the XUV radiation. Although multilayer mirrors can be used to select one harmonic order, the contrast ratio of reflectivity is sometimes poor. On the other hand, a grating monochromator gives high spectral purity of the selected radiation, but it introduces a stretch of the pulse duration due to the pulse-front tilt. This effect may compromise the ultrafast time resolution and high peak intensity when HHs are selected through a single-grating monochromator [7, 8].

A possible approach to overcome these drawbacks is the so called *time-delay compensated monochromator* (TDCM) [9–11]. It consists of a pair of gratings mounted in two stages to compensate for the pulse-front tilt: the first one acts as a traditional single-grating monochromator with an exit slit that performs the spectral selection of a single harmonic order, the second one is designed to compensate the temporal and spectral stretching introduced by the first grating. Both on-plane (classical) [12–14] and off-plane (conical) [15–17] configurations have been used for the realization of such a type of devices. In particular, the optical design that was originally proposed in Ref. 9 and later realized as described in Refs 13 and 14, consists of two toroidal gratings at moderate grazing incidence (142° subtended angle) that have been demonstrated to perform the selection of a single harmonic at 38 nm with a temporal duration of 11 ± 3 fs.

In this paper we propose the use of active gratings to realize a TDCM. The main advantage of using an active grating with respect to a conventional one is the possibility to choose the best included angle for matching the operation in the spectral interval of interest (e.g. the diffraction efficiency and/or the resolution) while maintaining fixed entrance and exit arms, since the radius of the grating is changed to maintain the system in the best focusing condition while scanning the wavelength. Furthermore, it is possible to use different geometries (e.g. different lengths of the entrance/exit arms to achieve different resolutions)

#185565 - $15.00 USD Received 19 Feb 2013; revised 11 Mar 2013; accepted 11 Mar 2013; published 20 May 2013

without changing the gratings, which are usually the most expensive components of the monochromator. The realization of active diffraction gratings has been extensively reported in the literature for a wide set of applications, ranging from telecommunication [18, 19] and optical displays [20] in the visible to synchrotron radiation beamlines in the soft X-rays [21, 22].

The optical components that we developed consist of a bimorph deformable mirror on the top of which a diffraction grating with laminar profile is realized by UV lithography. The gratings are voltage-controlled devices, where the voltage that is applied to the piezo-actuator controls the radius of curvature of the spherical surface. The grating realization and characterization are extensively described in [23]. Beyond the flexibility to use the same grating in different geometries by changing the radius of curvature and the capability of fine adjustment, another advantage of the active gratings here described is the very low cost of realization compared to a conventional grating ruled on a bulk substrate.

The scheme of the TDCM is based on the use of two active gratings in grazing-incidence. We demonstrate the ability of this device to achieve spectral selection while compensating for the pulse-front tilt. The experimental proof of principle has been performed in the near infrared with a Ti-Sapphire laser at 800 nm, since at this wavelength the spatial, spectral and temporal characterization of the light pulses are easily achieved. The feasibility of a TDCM for the spectral selection of HHs in the XUV is demonstrated by ray-tracing simulations.

2. Optical set-up

The setup of the monochromator consists of an entrance slit, an intermediate slit and two active gratings placed as shown in Fig. 1. The design parameters are listed in Table 1.

Table 1. Parameters of the monochromator

$p_1 = q_2$	mm	300
$q_1 = p_2$	mm	500
$K = \alpha_1 + \beta_1 = \alpha_2 + \beta_2$	deg	155
groove density	mm^{-1}	25
Radius and applied voltage @800 nm	mm, V	1850, 150
Grating diameter	mm	15

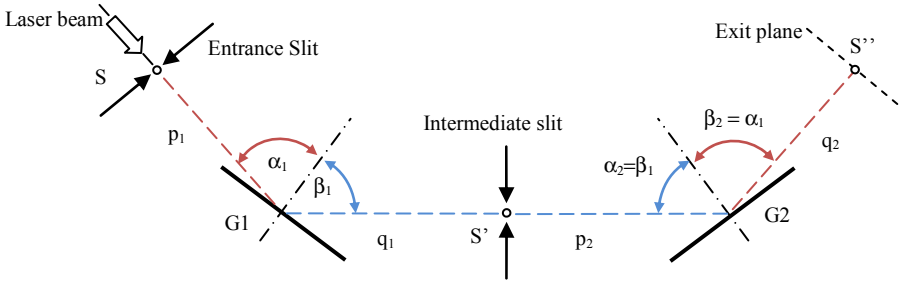

Fig. 1. Schematic of the TDCM monochromator: S is the source, S' the image of S in the intermediate plane, that is the focal plane of G1; S" is the image of S' at the exit plane, that is the focal plane of G2; $p_{1,2}$ and $q_{1,2}$ are respectively the lengths of the entrance and exit arms of G1,2; $\alpha_{1,2}$ and $\beta_{1,2}$ are respectively the incidence and diffraction angles.

The wavelength selection is performed through the rotation of the gratings, following the equations

$$\alpha_1 = \frac{K}{2} + \mathrm{a}\sin\left[\frac{m\lambda\sigma}{2\cos(K/2)}\right],\ \alpha_2 = \frac{K}{2} - \mathrm{a}\sin\left[\frac{m\lambda\sigma}{2\cos(K/2)}\right] \qquad (1)$$

#185565 - $15.00 USD Received 19 Feb 2013; revised 11 Mar 2013; accepted 11 Mar 2013; published 20 May 2013

where K is the subtended angle, λ the wavelength, σ the grating groove density and *m* the diffraction order of G1. G1 is rotated to diffract and focus the desired wavelength on the intermediate plane, G2 is consequently rotated to focus the radiation at the exit plane and compensate for the pulse-front tilt given by G1. The grating radii R_{G1} and R_{G2} have to be modified according to the equation

$$R_{G1} = R_{G2} = \left(\cos\alpha_1 + \cos\beta_1\right)\left(\frac{\cos^2\alpha_1}{p_1} + \frac{\cos^2\beta_1}{q_1}\right)^{-1} \qquad (2)$$

which is the condition to cancel the spectral defocusing. The groove density is constant, therefore, when the surface is bent according to Eq. (2), the groove density will also be changed. It can be calculated that the variation of the total length of the surface induced by the piezo-actuator when changing from a plane to a sphere with a curvature of few meters is about 10 um for a grating that is 15-mm long. Therefore, the effect on the variation of the groove density is totally negligible.

The configuration has been tested in the near infrared with a Ti-Sapphire laser source operated at 800 nm with a pulse length of 60 fs. The compensation of the pulse-front tilt requires that the two stages of the monochromator are operated in opposite orders, either (G1 internal/G2 external) or (G1 external/G2 internal). Among them, the configuration that has been realized is the (G1 internal/G2 external) because it reduces the vignetting (defined as the ratio between the number of rays that do not reach the exit plane, and the total number of rays from the source S)operated by G2 on the beam dispersed by G1. In fact, the dispersion in the intermediate plane, that is defined as $\delta l/\delta\lambda = \sigma q/\cos\beta_1$ (l is the displacement at the grating focal plane caused by a wavelength change of δλ), is bigger when G1 is used in the external order. Consequently, the footprint of the dispersed beam on G2 is larger for the external order, thus increasing the vignetting.

The spectrum of the laser source and the vignetting calculated for both configurations are shown in Fig. 2. The profiles of the focal spot in the intermediate plane and in the exit plane are shown in Fig. 3. The higher dispersion in the intermediate plane is quite evident for the external order (see Fig. 3b).

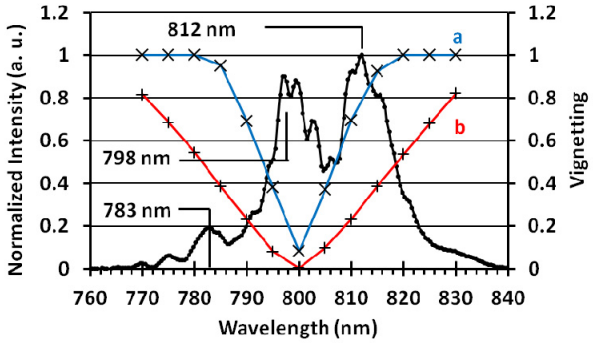

Fig. 2. Spectrum of the laser source and vignetting operated by G2. The spectrum is plotted in continuous black line. The vignetting factor is plotted for both the configurations: a) G1 internal/G2 external and b) G1 external/G2 internal.

#185565 - $15.00 USD Received 19 Feb 2013; revised 11 Mar 2013; accepted 11 Mar 2013; published 20 May 2013

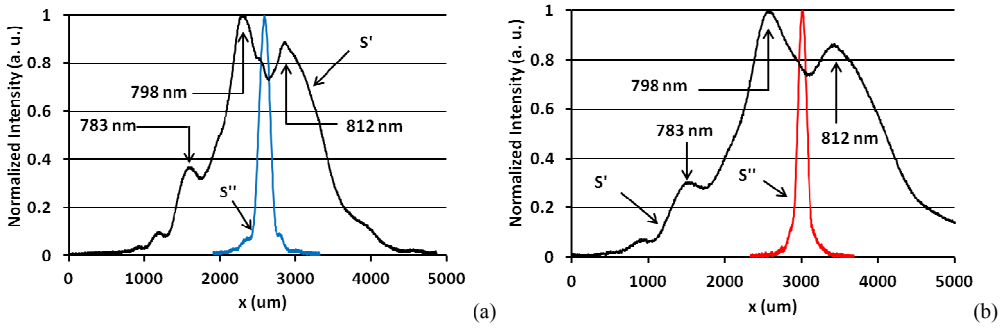

Fig. 3. Focal spot in the intermediate plane (S') and in the exit plane (S"): (a) G1 internal/G2 external; (b) G1 external/G2 internal.

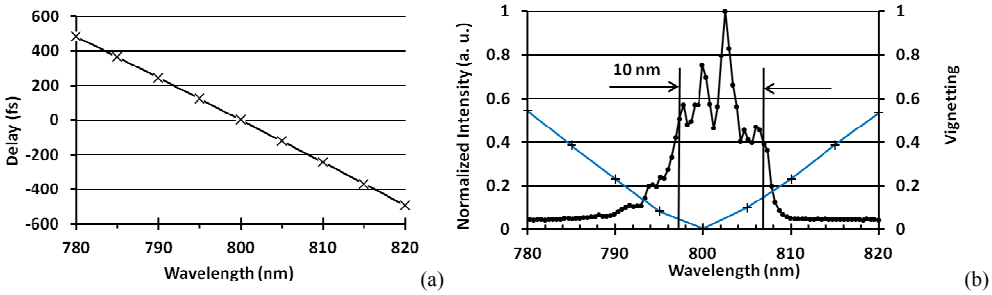

Fig. 4. (a) GD introduced by the monochromator in the 780-820 nm waveband. (b) Laser spectrum limited by the intermediate slit and associated vignetting given by G2.

The monochromator introduces a group delay (GD) within its range of operation. This effect, although expected to be negligible in the XUV spectral domain, is quite important in the near infrared. The GD added by the monochromator as calculated from ray-tracing is shown in Fig. 4(a): it consists of about 600 fs in the range between 785 nm and 810 nm. In order to reduce the pulse broadening due to the GD and the vignetting operated by G2, the laser spectrum has been limited to 10 nm using the intermediate slit, as shown in Fig. 4(b). The corresponding vignetting is limited to 0.1 and the GD is 200 fs. Since the Fourier limit duration for a 10-nm-wide pulse centered at 800 nm is 90 fs and the broadening due to the grating residual aberrations is expected to be less than 20 fs from ray-tracing simulations, the expected temporal broadening is globally about 220 fs.

3. Results

To validate the operation of the optical configuration, the temporal broadening and the pulse-front tilt have been measured. The incidence angles on the two gratings have been chosen in agreement with Eq. (1) to perform the wavelength selection on the intermediate slit. The voltage on the two piezo-actuators has been chosen to achieve a curvature of the spherical surface in accordance to Eq. (2) for the spectral focusing.

3.1 Temporal broadening

Figure 5 shows the FROG traces of the output pulse, carried out using a SHG FROG [24]. The pulse duration has been measured to be 220 fs in the exit plane, in good agreement with the expected temporal broadening.

#185565 - $15.00 USD Received 19 Feb 2013; revised 11 Mar 2013; accepted 11 Mar 2013; published 20 May 2013

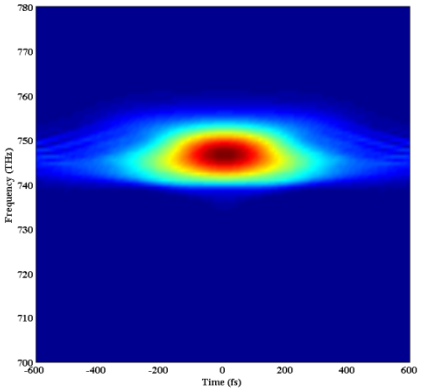

Fig. 5. FROG trace of the output pulses.

3.2 Pulse-front tilt measurements

The compensation of the pulse-front tilt operated by the TDCM has been demonstrated using a Michelson interferometer in which one arm is equipped with an additional folding mirror [25]. The operation of a standard Michelson interferometer on a pulse with front-tilt Δt is shown in Fig. 6(a). The two arms act symmetrically on the pulse and the interference fringes appear uniformly at the output on the whole beam spot. On the other hand, the modified configuration presented in Fig. 6(b) flips the left and the right side of the pulse in one arm of the interferometer and the fringes are observed only in the portions of the two pulses that are overlapped. The measurements are shown in Fig. 7. The upper row refers to the non-compensated (G1 internal/ G2 zero-order) configuration. As can be clearly seen in the figure, by changing the delay between the two arms of the interferometer, one observes the interference fringes moving along the section of the beam. This is a clear indication of the presence of pulse-front tilt, that is expected to be about 1 ps in good agreement with the experimental results. On the other hand, the compensated configuration (G1 internal/G2 external) does not show any pulse-front tilt; indeed as shown in lower row of Fig. 7, the intensity of the interference pattern is modulated as a function of the interferometer delay but the fringe envelope does not change position with the delay.

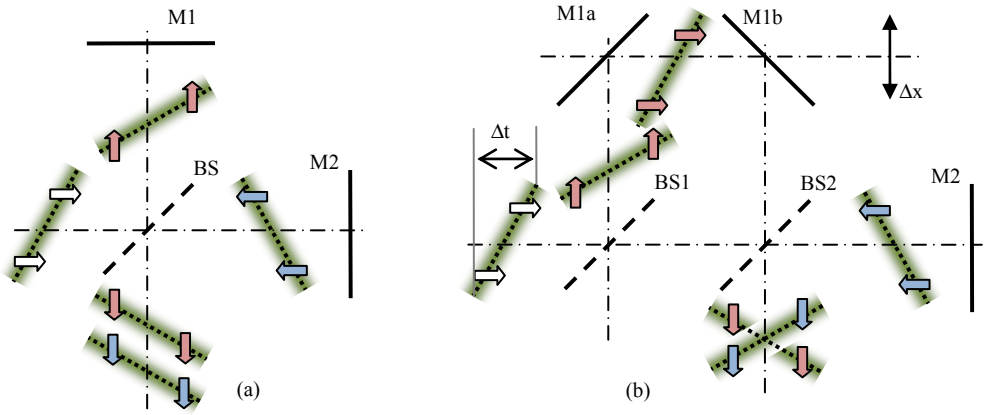

Fig. 6. Comparison between a standard Michelson interferometer (a) and the modified version used to measure the pulse-front tilt (b).

#185565 - $15.00 USD Received 19 Feb 2013; revised 11 Mar 2013; accepted 11 Mar 2013; published 20 May 2013

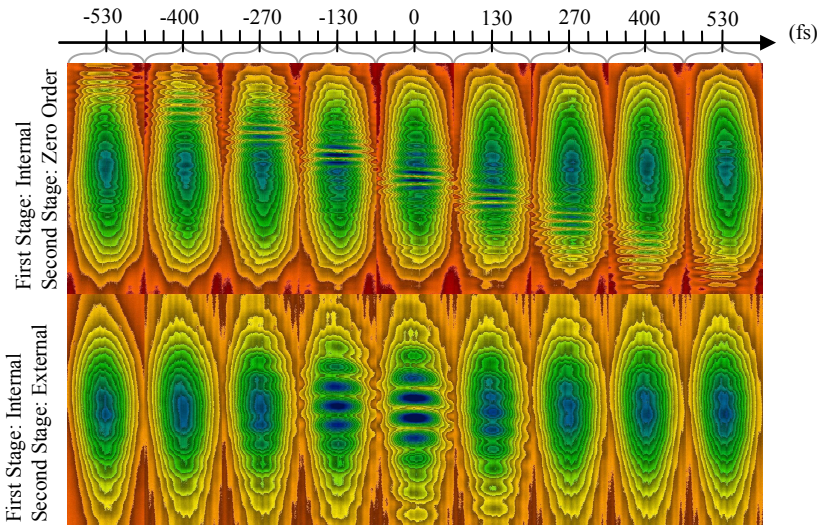

Fig. 7. Interference fringes acquired using the interferometer for front-tilt detection. Upper row: non-compensated configuration. Lower row: compensated configuration.

4. Application to extreme-ultraviolet high-order harmonics

The design of a TDCM for the selection of HHs in the region 20 – 80 nm (H_{39} – H_{11} with H_1 = 800 nm) is here presented. The optical layout is shown in Fig. 8. The system consists of three optical elements, namely two spherical gratings and a toroidal mirror. The gratings are operated in the time-delay compensated configuration already shown in Fig. 1. Since a spherical surface at grazing incidence focuses the beam only in its tangential plane and has no focusing capabilities in its sagittal plane, the spot at the output of both gratings is astigmatic, i.e. it appears as a vertical line that is focused only in the spectral dispersion horizontal plane. With reference to Fig. 8, a stigmatic spot is finally provided by an additional toroidal mirror (TM) that conjugates S”’ with S in the spatial plane and S”’ with S” in the spectral plane. The mirror radii are calculated by

$$\frac{1}{p_M}+\frac{1}{q_M}=\frac{2}{R\cos\gamma},\quad \frac{1}{2p+2q+p_M}+\frac{1}{q_M}=\frac{2\cos\gamma}{\rho} \tag{3}$$

where R and r are respectively the tangential and sagittal radii. The optical parameters of the configuration are presented in Table 2.

Table 2. Parameters of the XUV monochromator

Spectral region of operation	nm	20-80
Accepted angle	mrad	6
Grating arms p = q	mm	300
Grating subtended angle	deg	160
Grating groove density	mm^{-1}	300
Grating diameter	mm	15
Mirror arms $p_M = q_M$	mm	500
Toroidal radii	mm	9550 - 41.5
Incidence angle γ	deg	87
Mirror size	mm	60 × 10

#185565 - $15.00 USD Received 19 Feb 2013; revised 11 Mar 2013; accepted 11 Mar 2013; published 20 May 2013

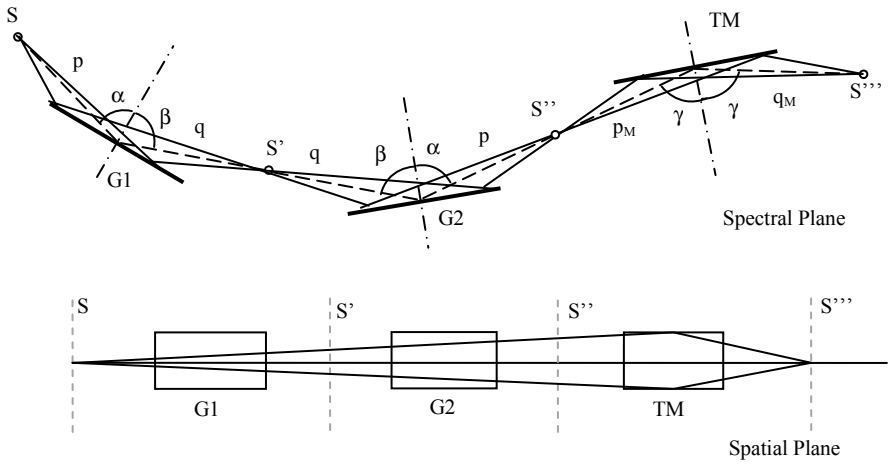

Fig. 8. Optical layout of a TDCM for the XUV spectral region. The spectral plane is the plane of the spectral dispersion. The spatial plane is the plane perpendicular to the spectral dispersion.

The variation of the grating radius and the grating rotation are shown in Fig. 9. The values of the curvature are well within the capabilities of the devices that have been realized, since the curvature may be changed from plane to 1.3 meters.

The performance of the monochromator have been calculated by ray-tracing simulations. The GD introduced by the monochromator is shown in Fig. 10(a): differently from the application in the IR spectral region, the delay is dramatically reduced, being less than 5 fs in the whole 20-80 nm spectral band. It can be concluded that the GD contribution within the bandwidth of a single harmonic selected by the monochromator is fully negligible in the femtosecond time scale. The wavefront distortions that contribute to the residual time broadening of the output pulse are shown in Fig. 10(b), that represents the ultimate time response of the monochromator. The residual aberrations are about 10 fs at 80 nm and lower at short wavelengths. The spot size at the mirror output is calculated to be 160 um × 100 um.

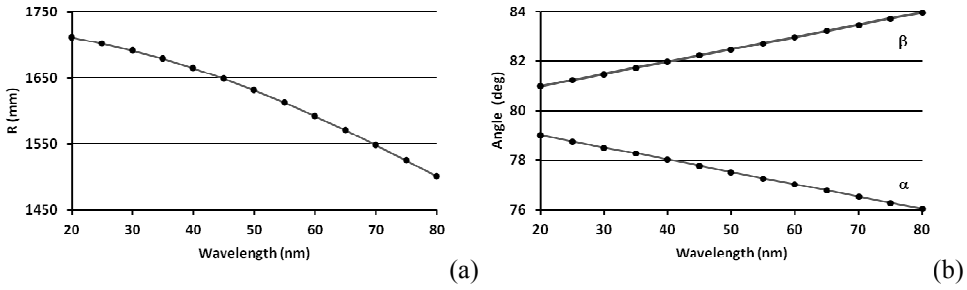

Fig. 9. Variation of the grating parameters with the wavelength: (a) radius; (b) incidence and diffraction angles.

#185565 - $15.00 USD Received 19 Feb 2013; revised 11 Mar 2013; accepted 11 Mar 2013; published 20 May 2013

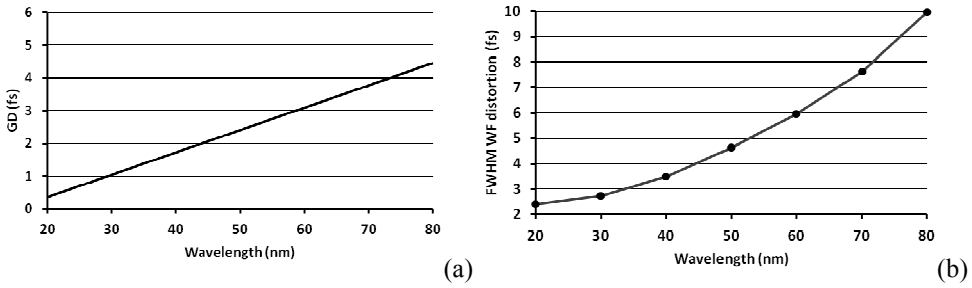

Fig. 10. Temporal response of the monochromator: (a) group delay, (b) wavefront distortion.

The main advantage of such a configuration with active gratings is the great flexibility to choose the parameters, such as the included angle and the arms, that better match the performance in the spectral interval of operation. Indeed it is possible to increase/decrease the length of the monochromator arms to achieve higher/lower spectral resolution without changing the gratings. Furthermore, active gratings, that are realized on a plane substrate, are definitely less expensive than conventional gratings realized on toroidal surfaces.

5. Conclusions

The experimental characterization of a TDCM realized with two active gratings operated at grazing incidence has been presented. The compensation of the pulse-front tilt has been demonstrated with ultrashort laser pulses at 800 nm and confirms the utility of active diffraction gratings for application to the spectral selection of ultrafast pulses in HH beamlines. Finally, the design of a XUV monochromator based on active gratings has been presented. The next development steps include the tests of the active gratings with HH XUV pulses.

Acknowledgments

We acknowledge partial financial support from the European Union within Contract no. 228334 JRA-ALADIN (Laserlab Europe II) and contract no. 307964 ERC StG – UDYNI and from the Italian Ministry of Research and Education (ELI project - ESFRI Roadmap).

#185565 - $15.00 USD Received 19 Feb 2013; revised 11 Mar 2013; accepted 11 Mar 2013; published 20 May 2013